Green synthesis of nanoparticles in cocos nucifera using aluminium nitrate nanohydrate with biomedical application and food preservative container

Yuvaraj Tamilselvi
Bharath Institute of Higher Education and Research
Moorthy Muruganandham
Bharath Institute of Higher Education and Research
Kanagasabapathy Sivasubramanian
Bharath Institute of Higher Education and Research
Dhakshan Prakash Vijayalakshmi
Bharath Institute of Higher Education and Research
Tamilselvan Amirthalingam
Bharath Institute of Higher Education and Research
Daram Sairam Reddy
Bharath Institute of Higher Education and Research
Avula Madhav
Bharath Institute of Higher Education and Research
Jeyanthi Rebecca
Bharath Institute of Higher Education and Research
Poorni Santhana Krishnan
Bharath Institute of Higher Education and Research
Rajkumar Sivanraju
rajkumar@hu.edu.et

Hawassa University
Palanivel Velmurugan
Bharath Institute of Higher Education and Research

Research Article

Keywords: Cocos nucifera, Aluminium nanoparticles, Antibacterial, Antioxidant, MIC, MBC, Biofilm, Food preservative container

Posted Date: June 6th, 2025

DOI: https://doi.org/10.21203/rs.3.rs-6652548/v1

Additional Declarations: No competing interests reported.

Version of Record: A version of this preprint was published at Discover Nano on July 28th, 2025. See the published version at https://doi.org/10.1186/s11671-025-04318-3.

Abstract

The article delves into the concept of green synthesis, a novel approach that harnesses *cocos nucifera* pollen extract and aluminium nitrate nanohydrate to produce aluminium nanoparticles (Al NPs). The findings suggest that Al NPs were successfully created with customizable properties, making them ideal for use in food applications. The techniques used to characterize the nanoparticles' structure and composition are highly intricate, revealing a unique resonance spectrum at 281 nm for the Al NPs in the ultraviolet-visible spectra. The Fourier transform infrared analysis showed that the *cocos nucifera* pollen extract contained functional groups of biomolecules. These biomolecules not only reduced the Al NPs but also served as capping agents. According to the HRTEM analyses, the nanoparticles exhibited a spherical shape, were densely packed, and had a size range of 100 nm to 10 nm. In X-ray energy diffraction, the Aluminium (Al) content accounted for 56% of the weight, and the X-ray diffraction analyzed the presence of a face-centred cubic crystalline structure in the formed Al NPs. A dose-dependent profile was observed in the antioxidant activity of the Al NPs, with a significant IC50 value of 43.17%, highlighting their effectiveness in scavenging radicals. The test strains of *S.aureus* and *E. coli* were significantly inhibited by the antibacterial properties of the Al NPs. When determining the lethal dose at 10^{-5}, the Minimal Inhibitory Concentration and Minimal Bactericidal Concentration are crucial factors to consider. The biofilm inhibition of *Escherichia coli* (72.46%) compared to staphylococcus *aureus* (48.55%). The green synthetic nanoparticles occur in food preservation so, the previously mentioned antimicrobial properties to food packaging material can be used as an impressive example. By controlling the spoiling rate of packaged food products and choosing reusable resources, this approach conforms with the environmentally friendly approaches in the food industry. This article summaries the huge potential of Al NPs innovations in maintaining sustainability in food packaging purposes to prevent food spoilage.

Introduction

Nanotechnology has enabled many developments, especially in the field of medicine and biotechnology, by the use of the special properties of nanoparticles (NPs) [1]. The traditional ways of NP synthesis are still working with hazardous chemicals and harsh conditions which create an environmental problem [2]. So, as a result of that, green synthesis methods have come into existence as sustainable methods, which use natural sources like plant extracts, microbes and biopolymers [3].

The green synthesis methods not only address the environmental issue but also have the benefits over the traditional methods [4]. Cutting down the energy consumption and the production of toxic byproducts contributes to the more sustainable manufacture of the products [5, 6]. Besides, the scalability of the green synthesis methods provides the possibility of their application in industrial production lines. The best way to achieve green synthesis at present is to use an extract from *Cocos nucifera* pollen and aluminium nitrate nanohydrate to produce nanoparticles for various uses. The coconut palm *(Cocos nucifera*) is a plant that is considered a valuable one in traditional medicine, culinary practices and cosmetics [7]. Its pollen contains many bioactive compounds and antioxidants, is

a very useful reducing agent and strengthens the body in nanoparticle synthesis. Contrary to aluminium nitrate, aluminium nitrate nanohydrate is a promoter of the start and the development of nanoparticle creation [8]. The use of *Cocos nucifera* pollen extract in NP synthesis is geared toward the principles of green chemistry, which is the concept that stresses renewable resources and benign solvents. This solution not only lessens the environmental impact but also enjoys the advantages of being cost-effective, scalable and bio-compatible. Besides, the pollen extract of *Cocos nucifera* possesses natural antioxidant and antimicrobial properties that enable the synthesis of the nanoparticles to be improved. Consequently, they are good for different applications in the medical and biotechnology fields [9]. This article offers a full review of the green synthesis of nanoparticles with the aid of aluminum nitrate nanohydrate and *Cocos nucifera* pollen extract. The information derived from the natural product research for the antioxidant and antibacterial activities data allows a setup of the low concentrations of Minimum Inhibitory Concentration (MIC), Minimum Bactericidal Concentration (MBC), and biofilm inhibition. The idea revolves around the use of nanoparticles as the main element that is green-synthesised to provide a solution to the regarded issues and challenges. FTIR, which is a Fourier-transform infrared spectrum, indicates the identification of the functional groups of nanoparticles [10]. XRD serves for phase identification and crystal structure confirmation of nanoparticles. TEM and EDS are employed given their capacity for analyzing both visible and surface morphology; highly sophisticated microscopy tools are used for the exploration of nanomaterial properties [11]. The performance in antioxidant properties is determined by the use of two DPPH and ABTS assays that provide a measure of the capability of nanoparticles in binding and thereby destroying free radicals [12]. Bacterial cultivation in agar plates and determination of MIC/MBC, quantitative tests are some of the tools used to test antibacterial activity. The findings display the viability of nanoparticles to serve as an innovative adjuvant to overcome multidrug resistance, which is a common problem in the present antibacterial treatment. Nanoparticles play a role in not only inhibiting the attachment and modulation of cell density but also in keeping the protein and mechanical properties of the cell unchanged.

The nanoparticles that are produced by green synthesis methods, especially those of aluminium, have great potential for a lot of applications, such as food preservation. The use of nanoparticles in food preservative containers is a method of devising containers which have strong antimicrobial properties and, at the same time, the packaging materials are sustainable [13]. The green synthesis methods, like the use of *Cocos nucifera* pollen extract with Aluminium nitrate nano-hydrate to produce nanoparticles, are a sustainable way of producing nanoparticles. Figure 1 showcases the process of biosynthesised AlNPs through the utilisation of *Cocos nucifera* extract.

This green process has reduced the impact on the environment. It made the synthesised nanoparticles biocompatible and safe for food contact applications. Aluminium nanoparticles, which are in the food preservative containers, have antimicrobial properties that are useful for the extension of the shelf life of the packaged food products. These nanoparticles can stop the multiplication of spoilage microorganisms and pathogens, and thus, food safety will be improved and food wastage will be lowered [14]. The use of green-synthesised aluminium nanoparticles in the containers of food preservatives is following the growing requirement for sustainable packaging solutions in the food

industry. The technology is employed to diminish the usage of conventional preservatives and to encourage eco-friendly materials, which in turn, helps in environmental conservation. In addition, the scalability of the green synthesis methods makes it possible to produce aluminium nanoparticles on a large scale, which can then be used for food packaging on a large scale. The increase in scalability with the cost-effectiveness of green synthesis approaches makes them commercially viable products in the food industry [15, 16].

Materials and Methods

2.1 Materials

The *Cocos nucifera* pollen used for the preparation of the plant extract was collected from cultivated coconut trees located in Padur village, Chennai, Tamil Nadu, India (Latitude: 12.8405° N, Longitude: 80.2248° E). Aluminium nitrate nano hydrate of molarity 0.37gm was utilized, for pH balancing hydrochloric acid and sodium hydroxide were used. Muller Hinton agar, Brain Heart Infusion Agar, crystal violet purchased from Sisco Research Laboratories Pvt. ltd.

2.1.1. Plant extract production

The *Cocos nucifera* pollen samples were checked for damaged discolouration, disease, etc. The pollen sample of *Cocos nucifera* pollen, 120 g, was weighed in a beaker. The distilled water of 600 ml was heated (100 ° Celsius) in a heating mantle till the water boiled. After boiling, 120 g of pollen samples were added for extraction. The plant extraction sample was removed from the mantle when it reached approximately 300 ml [17].

2.1.2 Metal solution preparation

Aluminium nitrate nano hydrate $Al(N0_3)_3.9\ H_20$ of morality 1 was used for the preparation of the metal solution. The molecular weight of aluminium nitrate nano-hydrate was 375.13 g/mole. The metal solution is prepared by adding 0.375 g dissolved in 100 ml of distilled water. The metal solution is kept in a magnetic stirrer for 30 min.

2.2 Methods

2.2.1 Optimization of extract

The extract of the plant sample (100 ml) was placed in a conical flask. The metal solution was prepared by adding 0.375 g of metal to 100 ml of distilled water and then transferring it to a 50 ml burette. The rate of metal solution added to the sample was set at 1 drop per 5 seconds, and the temperature was maintained at 50 degrees Celsius [18]. The time of colour change was recorded, and further colour changes were observed with the burette and time readings.

2.2.2 Optimization of pH

The plant sample extract (50ml) is added with metal until the colour changes. In Fig. 2.1, the ideal pH of the substrate is indicated. The pH set form (4 to 11) the optimism of pH is noticed from UV spectroscopy.

2.2.3 Optimization of *cocos nucifera* pollen sample extract

In the plant sample extract, a metal ratio of 9:1,19:1,29:1,39:1,49:1 is set by keeping the metal in the same concentration. UV spectroscopy of the optimum plant sample extract-metal ratio obtained in Fig. 2.2.

2.2.4 Optimization of metal

The metal, plant sample extract ratio is configured as follows: 0.25:39, 0.50:39, 0.75:39, 1.0:39, 1.25:39, 1.50:39, 1.75:39, and 2.0:39. The metal's optimism of metal solution obtained as shown Fig. 2.3.

2.2.5 Optimization of time

The *cocos nucifera* pollen sample extract of 39 ml of optimised pH is added with 1.75 ml of metal and is subjected to UV spectroscopy for a Time interval of 5 min The reading is taken from 0 to 25 min. The optimism of time is 15 minutes.

2.2.6 Bulk production

The sample underwent bulk production with optimised pH, plant sample extract, metal, and time readings. The bulk production setup involved placing the sample in a 2500 ml jar and keeping it on a magnetic stirrer. The metal solution was mixed by adding drops by drop to the sample at regular 5-second intervals. 1910.25 ml of *Cocos nucifera* pollen extract sample was combined with 89.735 ml of metal solution for 24 hours. After 24 hours, colour changes were noted, and the substrate was dried in a hot air oven at 80 degrees Celsius.

2.2.7 Calcination

The dried substrate was removed from the beaker as powder or crystals and kept in a heat furnace. The dried sample was kept in a crucible and calcined in furnaces for 2 hrs at 800 degrees Celsius at calcination. The sample was cooled down for 24 hrs [19].

2. Characterisation of AlNPs

3.1 Thermogravimetric Analysis (TGA) Procedure

A small amount (5-10mg) of greyish nanoparticle powder, resembling fine ash, was carefully spooned into a pristine, new alumina crucible. The powder, a subtle grit against her gloved fingers, was loaded into the gleaming Toledo TGA/SDTA851e apparatus for analysis; the sterile air smelled faintly of ozone. To prevent oxidation within the TA Instruments Q50, a continuous nitrogen purge (20–50 mL/min)

created a stable, inert atmosphere for the experiment [20]. The nanocomposite's resistance to high temperatures was analyzed through TGA, gradually heating a 5–10 mg sample from room temperature to 800°C at 10°C/min in a nitrogen environment.

3.2 FTIR Spectral Analysis

To begin the process of analysing aluminium nanoparticles with the help of FTIR, you have to first disperse the nanoparticles in a suitable solvent like ethanol, and then make sure that the solvent and nanoparticles are thoroughly mixed to obtain a homogeneous suspension [21]. In the first phase, a suspension is coated onto an FTIR-compatible substrate. Subsequently, a small drop of the suspension is laid onto the substrate. Measures should be implemented to make sure that the solvent has completely evaporated, thereby the spectral acquisition will not be affected. Subsequently, the FTIR spectra are obtained within a wavelength span of 4000 to 400 cm^-1. The peaks of Al compounds are assigned according to the Al compound spectrum and may include the vibrations of Al-O, Al-OH and Al-H bonds, which reveal the surface chemistry and the functional groups on the nanoparticles.

3.3 XRD Analysis

To illustrate aluminium nanoparticles using X-ray diffraction (XRD), initially, you have to create a thin film or a powder of the nanoparticles. The uniform thin layer is deposited on a proper substrate for thin films, and the fine ground sample is a necessity for powders. After, put the sample in the XRD machine, which usually has a rotating stage for the nanoparticles to be in a random orientation. X-rays are aimed at the sample, and the obtained diffraction pattern, which is a combination of the peaks related to the crystal lattice planes, is recorded. The study of the peak positions and intensities provides data on the nanoparticle crystalline structure, for example, face-centred cubic (FCC) for aluminium. Besides, the crystallite size and strain can be found through the appropriate mathematical models. The most recent XRD tools technologies, for instance, the high-resolution detectors and the synchrotron radiation sources, have greatly enhanced the accuracy and sensitivity of nanoparticle analysis [22]. In addition to that, the applied data analysis methods, like the total pattern fitting and the Rietveld refinement, provide more options for the comprehensive characterisation of the complex nanoparticle systems, thus, the structural parameters can be obtained with a higher accuracy [23].

3.4 HR-TEM Examination of AlNPs

First of all, HRTEM, aluminium nanoparticles are to be described by the sample dispersion, which is not a problem. The sample dispersion is usually done by the method of drop-casting the diluted nanoparticle suspension onto a carbon-coated HRTEM grid. The solvent evaporates, and the grid is introduced to the HRTEM camera. HRTEM imaging perceives the morphological aspects at the micro level, for instance, the particle size, shape, and crystallographic features, at the atomic level [24]. Recently, the new HRTEM instruments like, for example, aberration correction and the development of the electron detectors, have increased the spatial resolution and the sensitivity, thus the nanoscale features can be observed with detail that was not possible in the past.

3. Application of synthesised AlNPs

4.1 Antioxidant activity

The 1,1-diphenyl-1,2-picrylhydrazyl (DPPH) method was utilised in testing for aluminium nanoparticles, derived from *Cocos nucifera* pollen extract, scavenging capacity [25]. A standard comprising ascorbic acid was prepared in separate test tubes containing various quantities of aluminum nanoparticles, that is, 20 µg/mL, 40 µg/mL, 60 µg/mL, 80 µg/mL, and 100 µg/mL. One ml of freshly made DPPH (0.1 mM) was transferred into each of the test tubes under intense mixing. For half an hour, the solution was kept in a dark place. As a control, 2 millilitres of ethanol was provided instead of aluminium nanoparticles, and the test was performed simultaneously [25]. The following formula was used to calculate the percentage DPPH radical scavenging activity of silver nanoparticles.

% DPPH Radical Scavenging Activity = [(Ao _ Ae)/Ao] * 100 …….. (1)

(Ao = optical density without extract; Ae = optical density with extract). The results were reported as IC50, which is the concentration of the sample required to inhibit 50% of the DPPH concentration.

4.2 Antibacterial activity

For this antimicrobial work, we used *Escherichia coli* and *S. aureus* bacterial strains by the agar well diffusion method. The notable colonies were cultivated in Luria-Bertani broth and the incubated medium was gently shaken for 24 hours using 200 rpm with a constant temperature of 37°C. Plates of LB agar was laid on. 100 µL of each culture from bacterial strain applied on each LB agar plate with the help of an L-shaped spreader's glass. plates were probed with a steel borer of 5 mm diameter as much as possible directly to the plate to inject 30µL of the aluminium nanoparticles into each of the drilled holes. At the temperature of 37°C, we kept them for 24 hours. Furthermore, the diameter was measured for inhibition zones in mm [26].

4.3 Minimum inhibitory concentration

The broth microdilution technique was applied to analyse the MIC of aluminium nanoparticles. Bacterial cultures were done in the nutrient broth at 37°C throughout the night. During this experiment, the nanoparticle solution of aluminium was dissolved in ethanol. Moreover, MHB was employed. A 96-well microtiter plate was utilised with 100 µL of MHB added to each well. In general, the second one was treated with 200 µL aluminium nanoparticles and subsequently diluted from dilution 2 to 10, using a 2-fold dilution method. This was immediately followed up by the addition of 50 µL of bacterial solution for the experimental wells (*E. coli* and *S. aureus*). The growth control well (11th well, which includes inoculum and MHB), negative control well (well number 1) and positive control (well number 12) were collected. The minimal concentration at which the growth wasn’t seen visually was taken as the nanoparticles’ MIC for the respective microorganism [27].

4.4 Minimum bacterial concentration

During MBC (Minimum Bactericidal Concentration) determination, a well experiments where no bacteria were evident were seen. When these wells were located, the contents were assigned to the clean petri plates and spread carefully. The plates were then placed in an incubation period lasting 18 hours at a temperature of 37 degrees Celsius, which was appropriately controlled. Such a stationary time led to bacterial growth, if extant, in the Petri plates. Later, the plates were carefully checked to determine the presence of colonies on them. Locating the MBC was through establishing the agar plate in which no bacterial colonies had grown or became numerous over the incubation period. Finally, this unique agar plate was the second one from the left and the one experimentally checked and documented as the one revealing the Minimum Bactericidal Concentration, an extremely important discovery [28, 29].

.

4.5 Antibiofilm activity

Aluminium nanoparticle-based anti-biofilm assays have great potential in addressing biofilm-associated infections and biofouling in clinical, food and water systems. These assays play a critical role in promoting innovative modalities to manage biofilms and enhance general well-being. The mechanisms of anti-biofilm action of aluminium nanoparticles against *E. coli* and *S. aureus* are of great importance for the development of novel strategies for biofilm control. Knowledge of the molecular and cellular interactions between the nanoparticle and the biofilm helps researchers pinpoint targets for intervention and improve the composition of nanoparticles to increase efficacy. *Staphylococcus aureus* and *Escherichia coli* are cultured for 24 hours. Following this, culture media (LB Broth) is prepared, inoculated (10µl per well), and incubated for another 24 hours. Next, Ethanol is used as a solvent to dilute the Al NPs [30]. The homogenized Al NPs is added to the biofilm-containing well at various concentrations (0.625 µl, 1.25 µl, 2.50 µl, 5.0 µl, 10 µl) that we were able to obtain in MIC, and the well is then incubated for 24 to 48 hours. Subsequently, the supernatant is cautiously extracted to avoid disrupting the biofilm. Following a 1% PBS cleaning, the wells are allowed to sit at room temperature for 15 to 30 minutes. Following a 15–30-minute incubation period, 0.1% crystal violet is added to the wells. After rinsing the wells, 150 µl of ethanol is added to help destain the biofilm. Then, at 570 nm, the OD is measured [31].

4.6 Food packaging material coating with Al_2O_3

The utilisation of nanomaterials in food packaging is widespread as they possess antimicrobial properties, offer UV protection, and have the potential to prevent oxidation. Frequently found in food packaging, nanoparticles are safe for human consumption and have been approved as food additives and for use in food contact materials [32, 33]. An aluminum sheet was coated with a sol-gel using nanoparticles, resulting in a sleek and durable finish. To start, we exactly mixed metal alkoxide and ethanol in a 1:4 ratio, forming the sol-gel solution with a smooth consistency. We slowly poured deionised water into the magnetic stirrer, feeling the coolness of the liquid as it made contact with the container. By employing a magnetic stirrer and stirring for at least 30 minutes, we achieved consistent dispersion throughout the mixture. Afterward, we allowed the sol-gel solution to sit undisturbed for approximately 24 hours, ensuring that hydrolysis and condensation were thoroughly carried out. After

washing the aluminum sheet to eliminate any dirt or grease, we patiently waited for it to air dry completely.

During the dip coating process, the aluminum sheet is submerged in the sol-gel solution and carefully pulled out at a controlled speed to achieve a uniform coating. We applied several concentration coats of each food container, giving each one enough time to dry before moving on to the next. After coating the aluminum sheet, we left it alone to air dry and let the solvent evaporate. Then, we carefully transferred the coated sheet into a drying oven, which we typically set to temperatures between 100°C and 300°C. Depending on the desired properties and the thickness of the coating, the curing time could vary from one hour to several hours [34]. We conducted experiments using a range of concentrations, from as low as 2.5 mg to as high as 160 mg. We started with 2.5 mg and gradually increased the concentrations by a factor of 2. Additionally, the antibacterial activity of the food container has been tested against *S. aureus* and *E. coli* using various concentrations of AlNPs .

Results

5.1 Optimisation of pH, Substrates, Time, and Precursor

Flavonoids, ketones, aldehydes, tannins, carboxylic acids, phenolics, and proteins are among the biomolecules found in plant extracts. These biomolecules are responsible for the transformation of Al^{+} to Al^{0}, leading to the synthesis of Al NPs. When it comes to these biosynthesised Al NPs, you can expect a variety of morphologies, diameters, and forms. These properties are significantly influenced by various experimental conditions, including time, pH, the kinetics of interaction between metal salts (Aluminium nitrate nano-hydrate) and reducing agents (coconut pollen), and the adsorption of capping agents.

Through the use of coconut pollen extract and response surface methodology, the study seeks to enhance the efficiency of green Al NPs synthesis. A key step in Al NPs synthesis is adding 50 ml of metal to the coconut pollen substrate until the colour undergoes a noticeable transformation. The substrate's pH was measured at 5, which falls below the ideal value of pH 7 (as shown in Fig. 3a). According to the UV-Vis spectra, it has been determined that the synthesis of Al NPs is unsuitable in acidic media with a pH between 1 and 5. Furthermore, one can observe a distinct lightening of the colour in the aluminum nanoparticle solution. Moreover, the nanoparticles' size is directly affected by the pH level. The Al NPs were synthesised at pH 7. When the environment is acidic, the particles tend to be larger in size, whereas in basic conditions, they are smaller [35].

Gontijo et al. (2020) note that the range of colours, spanning from colourless to yellow, is a result of the size effect, which is influenced by the pH level. By changing the pH of the reaction, biomolecules undergo a shift in their electrical charges, which directly impacts their ability to cap and stabilise, ultimately influencing the growth of nanoparticles. In alkaline media with pH 9 and 11, a noticeable color change occurred, yet the shift in characteristic peaks in the spectra did not suggest the presence of nanoparticles. Furthermore, the pH 11 condition resulted in observable agglomeration of nanoparticles.

The concentration ratios of coconut pollen vary, with the optimal substrate concentration being 39 milliliters, as shown in Fig. 3b. The range of ratios varies from 9:1 to 49:1, demonstrating a significant difference in values. With precision, the pH of the 39 ml substrate was calibrated to 7, ensuring optimal conditions for the experiment.

The metal optimisation process involves establishing different metal substrate ratios, such as 0.25:39, 0.50:39, 0.75:39, 1.0:39, 1.25:39, 1.50:39, 1.75:39, and 2.0:39. The metal optimisation has been fine-tuned to 1.75 ml, as shown in the accompanying Fig. 3c. The addition of 39 millilitres of pH 7 substrate and 1.75 millilitres of metal created a bubbling sound, as if the mixture was coming to life. The optimal time is determined to be 15 minutes (Fig. 3d).

The UV-Vis spectra analysis of Al NPs, synthesised using coconut pollen extracts, reveals a direct correlation between reaction time and absorption peak intensity. A noticeable trend emerges as the reaction time progresses from 0 to 20 minutes, with the absorption peak intensity consistently increasing. The plant-extract-synthesised Al NPs display prominent absorbance, as indicated by the surface plasmon resonance (SPR) peaks at 280 nm according to the spectra analysis. After 24 hours, the UV-Vis spectra displayed no alterations in absorbance, providing further evidence that the optimal reaction time was 15 minutes.

The synergistic effect of the bioactive components in the coconut pollen extract aids in the bio-reduction of Al^{+} ions, transforming them into Aluminium 0xide nanoparticles. By analyzing the absorption spectra, the ideal proportion of coconut pollen extract to aluminium nitrate solution can be identified to maximize the synthesis of aluminum nanoparticles.

5.2 Characterization

5.2.1 Thermogravimetric Analysis (TGA)

Three major degradation phases can be seen in the green-synthesised aluminum nanoparticles' TGA profile. When temperatures drop below 150°C, moisture and volatile organics evaporate, resulting in an initial weight loss of 2–4 per cent. A 10–20% loss is ascribed to the degradation of organic capping agents, including flavonoids and polyphenols, from the extract of Cocos nucifera between 200°C and 400°C. Between 400°C and 600°C, a significant 30–50% loss suggests that stable bioorganic residues are breaking down and that aluminum species are turning into aluminum oxide (AlO_3). Upon reaching 800°C, the curve stabilizes with a residual mass of 25–30%, indicating the development of a thermally stable Al_2O_3 core that is appropriate for high-temperature uses such as biomedical coatings and food packaging [36].

5.2.1 FTIR Analysis

The coconut pollen extract treated with $AlNO_3$ underwent FT-IR analysis to elucidate the bond linkages and functional groups involved. By conducting FT-IR analysis on the plant extract-based synthesised Al

NPs, the functional groups were determined. The confirmation of the phenol group was evident through the observation of a distinct band at 3410.12 cm – 1, indicating O-H stretching vibrations (Fig. 5). Bands at 2295.31 cm^{-1}, 2853.23 cm^{-1}, and 2359.54 cm^{-1} represent characteristic stretching bands of C-N, methyl group, and C-O bond. The Peaks at 1468.12 cm^{-1} and 1407.65 cm^{-1} correspond to nitrosamines and alkanes, respectively. The observed peaks suggest some electrostatic interactions between the Al NPs and functional groups of capping agents. In the FT-IR spectrum of Al NPs, a peak at 1117.41 cm^{-1} as well as an increase in the intensity of the peak at 1050.2$cm^{-1,}$ are attributed to alkyl amine vibrations, indicating that the reduction of the aluminium ions is due to the oxidation of the hydroxyl groups to the carbonyl groups in the plant extract. The peaks located at 865.24 cm^{-1} and higher are due to bending vibrations of C-H stretching bands. The characteristic absorption peaks due to bending vibrations of aromatics, amines, amides, and acids were observed at 674.24 cm^{-1}, 619.82 cm^{-1}, and 565. cm^{-1}. Chen and Mu's specified polyphenols shared a similar banding pattern in the functional group and fingerprint region. Based on the FT-IR investigation, it can be assumed that phenolic and flavonoid compounds present in the coconut pollen extract-based synthesized Al NPs may be involved in capping and stabilizing the nanoparticles [37]. The spectral application provides substantial information on the nanoparticle's surface modifications and their interactions, which are important for several applications, from catalysis to biomedical engineering. Finally, the processing of the FTIR spectra using data analysis methods such as peak integration and deconvolution can be used to deepen the understanding of the spectra, hence, the accurate characterization of aluminium nanoparticles is achieved.

5.2.2 HRTEM and XRD

HRTEM analysis showed well-dispersed, spherical-shaped nanoparticles ranging from 10 nm to 100nm in size. Figure 6 (a-d) depicts cubic aluminium nanoparticles with smooth surfaces dispersed evenly. The TEM image reveals a relatively narrow size distribution of the aluminium nanoparticles, with an average diameter of approximately 51nm.

The X-ray diffraction (XRD) analysis examined and verified the crystalline nature of Al nanoparticles. The XRD pattern of the dried nanoparticles obtained from colloid samples revealed peaks at 2 theta (θ) degrees of approximately 33.1°, 40.5°, 50.2°, 58.5°, 67.02°, and 73.5°, which could be associated with the (110), (113), (024), (116), (214), (300), and (311) facets, respectively (Fig. 7). These corresponded to the database of the Joint Committee on Powder Diffraction Standards (JCPDS), card No. 71-1683. The size of the nanoparticles was calculated using the Debye–Scherrer formula (Eq. 1)

The nanoparticles' crystalline size (D) can be calculated using the formula

$$D = K\lambda / \beta Cos\theta \quad \ldots\ldots\ldots\ldots\ldots (1)$$

where K is the Scherrer constant (0.98), λ is the wavelength (1.54), and β is the full width at half maximum (FWHM). The crystallite size of Al/AlO nanoparticles is 42.73 nm, which is consistent with the results from HRTEM images and previous studies by Adnan A. Mohammed in 2020. The unassigned peaks in the XRD pattern may be attributed to the crystallization of a bioorganic phase on the surface of

the nanoparticles. Overall, the XRD pattern clearly demonstrates that the aluminum nanoparticles synthesized are crystalline in nature [38].

5.3 Application

5.3.1 Antioxidant activity

Antioxidant activity is tested using a variety of mechanisms, including electron transfer (ET) and hydrogen transfer (HAT) from the antioxidant to free radicals. To compare antioxidant activity, ascorbic acid is employed as a standard. When the scavenging material is recognized as (metal), it neutralizes the free radical, which increases the intensity of the deep purple color. This shows that the metal acts as an antioxidant, effectively neutralising free radicals.

The antioxidant properties of aluminium nitrate nanoparticles were investigated using the DPPH method of assay. For positive control, ascorbic acid was employed, and the control OD obtained for ascorbic acid is 3.372, which is the same OD value as we acquired for the nanoparticles control OD [39]. Different nanoparticle concentrations produced different percentages of inhibition: 10.64% for 20 µl, 17.58% for 40 µl, 26.98% for 60 µl, 37.93% for 80 µl, and 43.17% for 100 µl. For ascorbic acid, the percentage of inhibition was found at different concentrations. The percentages are 9.01%, 12.15%, 15.42%, 24.61%, and 30.57%, respectively, for the various ascorbic acid concentrations (20 µl, 40 µl, 60 µl, 80 µl, and 100 µl) shown in Fig. 8a. Therefore, we conclude that aluminium nitrate nanoparticles positively affect antioxidant capabilities based on the inhibitory percentage results

5.3.2 Antibacterial activity

Aluminium nanoparticles were evaluated for their antibacterial activity against a variety of bacterial strains, including *Staphylococcus aureus* and *E. coli*. The results show that nanoparticles synthesised using the green method have effective antibacterial activity against pathogenic bacteria. The findings demonstrated that as the concentration of nanoparticles increased, so did their inhibitory effect (Fig. 10b). Figures 9a and b measured the inhibitory zone's diameter, indicating the microorganism susceptibility level. Table 1 shows the *E. coli* exhibit a large zone of inhibition [14mm in 50µl,16mm in 100µl,18mm in 150µl,20mm in 200µl,21mm in 250µl] compared to the *S.aureus* zone of inhibition [12mm in 50µl,13mm in 100µl,14mm in 150µl,15mm in 200µl,16mm in 250µl]. The result is more similar to the aluminium oxide nanoparticle's antibacterial activity, as the *E. coli* has a larger zone of inhibition compared to Proteus vulgaris [40]. Even after washing, the food container coated with AlNPs nanoparticles displayed significant inhibition against *E. coli* and *S. aureus*, showcasing its antibacterial properties. We treated the bacteria with a range of concentrations, from 2.5 mg to 160 mg, and observed the effects.

5.3.3 Minimum inhibitory concentration

After the incubation of 24 hours at 37 degrees Celsius, the 96 plate wells with 10 and 5 mg/ml concentrations that contain aluminium nanoparticles show the growth inhibition of bacteria [90.76% and

95.71% in *E. coli*, 65.46% and 71.17% in *S. aureus*] which is shown in Fig. 9b. It was clear that among all the other concentrations (10, 5, 2.5, 1.25, and 0.625 mg/ml), they had the strongest impact on inhibiting bacteria, with the MIC achieved at 0.625 mg/ml [41]. These results thus confirm that the aluminium nanoparticles have a measurable impact on the growth of *S. aureus* and *E. coli*.

5.3.4 Minimum bacterial growth

The suspensions from the 96-well plates showed no growth of bacteria at concentrations ranging from 10 to 0.625 mg/ml. To check the minimum bactericidal concentration (MBC), the control (without nanoparticles) and concentrations of 10 and 0.625 mg/ml were inoculated in agar plates and incubated for 24 hours. No growth was observed in both concentrations, while adequate growth was observed in the control (Fig. 10a and 10b). However, the other concentrations of nanoparticles (0.312, 0.156, 0.078, and 0.039 mg/ml) showed bacterial colonies. The MBC test helps determine the minimum concentration of nanoparticles needed to achieve a bactericidal effect. When 99.9% of the bacterial population is killed at the lowest concentration of an antimicrobial agent, it is termed an MBC endpoint. These observations confirm that the nanoparticles are bactericidal at a minimum inhibitory concentration (MIC) of 0.625 for both *S. aureus* and *E. coli* [42].

5.3.5 Anti-biofilm assay

In biofilm inhibition activity, there are several bacteria in the form of biofilm. Biofilms are ubiquitous, they form on virtually all surfaces immersed in natural aqueous environments. A biofilm shows certain properties to bacteria that are not seen in the planktonic state, a fact that justifies the recognition of dental plaque as a biofilm. Aluminium oxide nanoparticles harm bacterial cultures such as *Escherichia coli* (gram-negative bacteria) and *Staphylococcus aureus* (gram-positive bacteria). Biofilm is a leading threat to the environment, industry, and human health. Figure 10b show the biofilm activity of aluminium nanoparticles describes which are more effective in *Escherichia coli* (72.46%) compared to *Staphylococcus aureus* (48.55%). Aluminium nanoparticles have reacted with the cell membrane and entered the

5.3.4 Food package materials coated with Al_2O_3 NPs

Ensuring food safety heavily relies on the proper use of food packaging. It’s very important to prevent spoilage and contamination, boosting sensitivity through the facilitation of enzyme activity [44]. The harsh environment in functional foods often causes the bioactive compounds to break down and lose their activity, resulting in shorter shelf life. Promising results have been seen in coating the nanoparticles on Al_2O_3 food-grade containers made up of aluminium material to extend and guarantee the longevity of a food product. The well-coated aluminium nanoparticles (NPs) were analysed using the FESEM image, which confirmed the even coating of the NPs on the food container. The surface of the aluminum sheet was comparatively homogeneous and smooth before washing (Fig. 11a). Distinct clusters and roughness were seen during nanoparticle coating and washing (Fig. 11b), indicating that AlNPs were successfully deposited. Increased surface roughness and nanoparticle adhesion demonstrate a direct correlation between these morphological changes and improved antibacterial action.

Our investigation revealed the synthetic material's antioxidant and antibacterial qualities, underscoring its possible use in food preservation. Using a sol-gel dip-coating technique, aluminum sheets were successfully coated with aluminum nanoparticles (AlNPs) at different concentrations: 2.5 mg to 160 mg, as indicated in Table 1. For comparison, a control sheet devoid of AlNPs was also created. The coating grew increasingly homogeneous and dense as the concentration of AlNPs increased, and at higher concentrations (particularly 80 mg and 160 mg), it showed a noticeable metallic shine. These findings imply efficient nanoparticle deposition, which most likely played a role in the enhanced functional characteristics seen.

Conclusion

This research aimed at synthesizing green aluminum nanoparticles using aqueous extract of plant pollen of *Cocos nucifera* and aluminum nitrate nonahydrate. Green synthesis provides an environmentally friendly approach to the synthesis reactions, which involves avoiding the hazardous chemicals and causing minimal harm to the physical environment. The optimised synthesis parameters were obtained from a series of tests such as pH, substrate: metal ratio, metal concentration and the reaction time. An exploration of the prospects of these green synthesised aluminium nanoparticles was made, where special concentration given on their antioxidant and antibacterial activity. Based on the results, the extent of the antioxidant activity of the nanoparticles was proportional to the concentration of the nanoparticles that was tested for free radical scavenging activity. In addition, antimicrobial tests showed fairly good activity against both *E. coli and S. aureus* bacteria, though *E. coli* was noted to be more sensitive to the extract. The MIC and MBC for all the nanoparticles under study was also assessed to understand the efficacy of these nanoparticles in the effective inhibition and /or killing of bacterial cells. Furthermore, it has appeared that the described nanoparticles provide valuable anti-biofilm effects concerning both *E. coli and S. aureus* bacteria. Therefore, the result of this research implies the possibility of using green-synthesised Al nanoparticles in food preservative containers. If such nanoparticles are introduced into the coating of the container, the life span of the food that is packed could also be enhanced due to the reduction of microbial activities as well as oxidation. The approach therefore provided is environmentally friendly and socially acceptable for the preservation of the food items, hence decreasing instances of food wastage while enhancing the health of the people. The future research will aim at using these produced nanoparticles in coatings of food contact surfaces and assessing the effectiveness of the same in the actual storage environment.

Declarations

Declaration of competing interest

The authors declare that they have no known competing financial interests or personal relationships that could have appeared to influence the work reported in this paper.

Ethics Statements

Ethics approval and consent to participate:

Not applicable. This study did not involve any human or animal participants.

Consent for publication:

Not applicable.

Plant collection and permissions:

The *Cocos nucifera* pollen used in this study was collected from cultivated coconut trees located in Padur village, Chennai, Tamil Nadu, India (Latitude: 12.8405° N, Longitude: 80.2248° E). The plant material was collected from privately owned farmland with permission from the landowner. As *Cocos nucifera* is not an endangered or protected species and the material was not collected from forest land, no specific permits or licenses were required. The collection complied with all relevant local and national regulations.

Data availability statement:

The datasets generated and/or analysed during the current study are available from the corresponding author on reasonable request.

Acknowledgement

The authors thank the Vice-Chancellor and Dean of Bharath Institute of Higher Education and Research for providing the research facilities.

Authors contribution

Conceptualisation: Sivanraju. Rajkumar, Supervision: Palanivel Velmurugan, Writing – original draft: Yuvaraj Tamilselvi, Methodology: Moorthy Muruganandham, Investigation: Kanagasabapathy Sivasubramanian, Software: Dhakshan Prakash Vijayalakshmi, Tamilselvan Amirthalingam, and Daram Sairam Reddy, Data curation: Avula Madhav, Jeyanthi Rebecca, and Poorni Santhana Krishnan, Writing – review & editing: Palanivel Velmurugan,

References

1. Altammar, K. A. (2023). A review on nanoparticles: characteristics, synthesis, applications, and challenges. *Frontiers in Microbiology*, *14*. https://doi.org/10.3389/FMICB.2023.1155622
2. Arnold, B. (2022). Calcination: From Aluminium Hydroxide to Aluminium Oxide. *Rubies and Implants*, 65–66. https://doi.org/10.1007/978-3-662-66116-1_22
3. Buchman, J. T., Hudson-Smith, N. V., Landy, K. M., & Haynes, C. L. (2019). Understanding Nanoparticle Toxicity Mechanisms to Inform Redesign Strategies to Reduce Environmental Impact. *Accounts of Chemical Research*, *52*(6), 1632–1642. https://doi.org/10.1021/ACS.ACCOUNTS.9B00053/SUPPL_FILE/AR9B00053_SI_001.PDF

4. Cimolai, N. (2021). Pharmacotherapy for Bordetella pertussis infection. I. A synthesis of laboratory sciences. *International Journal of Antimicrobial Agents*, *57*(3), 106258. https://doi.org/10.1016/J.IJANTIMICAG.2020.106258
5. Coelho, A. A. (2018). Deconvolution of instrument and Kα2 contributions from X-ray powder diffraction patterns using nonlinear least squares with penalties: *Journal of Applied Crystallography*, *51*(1), 112–123. https://doi.org/10.1107/S1600576717017988
6. Flores, A. M., Hosseini-Nassab, N., Jarr, K. U., Ye, J., Zhu, X., Wirka, R., Koh, A. L., Tsantilas, P., Wang, Y., Nanda, V., Kojima, Y., Zeng, Y., Lotfi, M., Sinclair, R., Weissman, I. L., Ingelsson, E., Smith, B. R., & Leeper, N. J. (2020). Pro-efferocytic nanoparticles are specifically taken up by lesional macrophages and prevent atherosclerosis. *Nature Nanotechnology 2020 15:2*, *15*(2), 154–161. https://doi.org/10.1038/s41565-019-0619-3
7. Kumar, M., Ranjan, R., Dandapat, S., Srivastava, R., & Sinha, M. P. (2022). XRD analysis for characterization of green nanoparticles: a mini review. *Manoj Kumar, Rakesh Ranjan, Sukumar Dandapat, Rohit Srivastava, Manoranjan Prasad Sinha (2022). XRD Analysis for Characterization of Green Nanoparticles: A Mini Review. Global Journal of Pharmacy and Pharmaceutical Sciences*, *10*(1), 555779.
8. Guerra, F. D., Attia, M. F., Whitehead, D. C., & Alexis, F. (2018). Nanotechnology for Environmental Remediation: Materials and Applications. *Molecules : A Journal of Synthetic Chemistry and Natural Product Chemistry*, *23*(7). https://doi.org/10.3390/MOLECULES23071760
9. Gupta, N., Sharma, N., Mathur, S. K., Chandra, R., & Nimesh, S. (2018). Advancement in nanotechnology-based approaches for the treatment and diagnosis of hypercholesterolemia. *Artificial Cells, Nanomedicine, and Biotechnology*, *46*(sup1), 188–197. https://doi.org/10.1080/21691401.2017.1417863
10. Habeeb Rahuman, H. B., Dhandapani, R., Narayanan, S., Palanivel, V., Paramasivam, R., Subbarayalu, R., Thangavelu, S., & Muthupandian, S. (2022). Medicinal plants mediated the green synthesis of silver nanoparticles and their biomedical applications. *IET Nanobiotechnology*, *16*(4), 115–144. https://doi.org/10.1049/NBT2.12078
11. Johnson, A., & Uwa, P. (2019). Eco-friendly synthesis of iron nanoparticles using Uvaria chamae: Characterization and biological activity. *Inorganic and Nano-Metal Chemistry*, *49*(12), 431–442. https://doi.org/10.1080/24701556.2019.1661448
12. Krysa, M., Szymańska-Chargot, M., & Zdunek, A. (2022). FT-IR and FT-Raman fingerprints of flavonoids – A review. *Food Chemistry*, *393*, 133430. https://doi.org/10.1016/J.FOODCHEM.2022.133430
13. Liaqat, N., Jahan, N., Khalil-ur-Rahman, Anwar, T., & Qureshi, H. (2022). Green synthesized silver nanoparticles: Optimization, characterization, antimicrobial activity, and cytotoxicity study by hemolysis assay. *Frontiers in Chemistry*, *10*, 952006. https://doi.org/10.3389/FCHEM.2022.952006/BIBTEX

14. Maity, G. N., Maity, P., Choudhuri, I., Sahoo, G. C., Maity, N., Ghosh, K., Bhattacharyya, N., Dalai, S., & Mondal, S. (2020). Green synthesis, characterization, antimicrobial and cytotoxic effect of silver nanoparticles using arabinoxylan isolated from Kalmegh. *International Journal of Biological Macromolecules*, *162*, 1025–1034. https://doi.org/10.1016/J.IJBIOMAC.2020.06.215
15. Manikandan, V., Velmurugan, P., Park, J. H., Chang, W. S., Park, Y. J., Jayanthi, P., Cho, M., & Oh, B. T. (2017). Green synthesis of silver oxide nanoparticles and its antibacterial activity against dental pathogens. *3 Biotech*, *7*(1), 1–9. https://doi.org/10.1007/S13205-017-0670-4/METRICS
16. Manikandan, V., Velmurugan, P., Park, J. H., Lovanh, N., Seo, S. K., Jayanthi, P., Park, Y. J., Cho, M., & Oh, B. T. (2016). Synthesis and antimicrobial activity of palladium nanoparticles from Prunus × yedoensis leaf extract. *Materials Letters*, *185*, 335–338. https://doi.org/10.1016/J.MATLET.2016.08.120
17. Nissim, M., Iline-Vul, T., Shoshani, S., Jacobi, G., Malka, E., Dombrovsky, A., Banin, E., & Margel, S. (2023). Synthesis and Characterization of Durable Antibiofilm and Antiviral Silane-Phosphonium Thin Coatings for Medical and Agricultural Applications. *ACS Omega*, *8*(42), 39354–39365. https://doi.org/10.1021/ACSOMEGA.3C04908/ASSET/IMAGES/LARGE/AO3C04908_0014.JPEG
18. Parvekar, P., Palaskar, J., Metgud, S., Maria, R., & Dutta, S. (2020). The minimum inhibitory concentration (MIC) and minimum bactericidal concentration (MBC) of silver nanoparticles against Staphylococcus aureus. *Biomaterial Investigations in Dentistry*, *7*(1), 105. https://doi.org/10.1080/26415275.2020.1796674
19. Periakaruppan, R., Chen, X., Thangaraj, K., Jeyaraj, A., Nguyen, H. H., Yu, Y., Hu, S., Lu, L., & Li, X. (2021). Utilization of tea resources with the production of superparamagnetic biogenic iron oxide nanoparticles and an assessment of their antioxidant activities. *Journal of Cleaner Production*, *278*, 123962. https://doi.org/10.1016/J.JCLEPRO.2020.123962
20. Prasher, P., Singh, M., & Mudila, H. (2018). Silver nanoparticles as antimicrobial therapeutics: current perspectives and future challenges. *3 Biotech*, *8*(10), 411. https://doi.org/10.1007/S13205-018-1436-3
21. Rajiv, P., Bavadharani, B., Kumar, M. N., & Vanathi, P. (2017). Synthesis and characterization of biogenic iron oxide nanoparticles using green chemistry approach and evaluating their biological activities. *Biocatalysis and Agricultural Biotechnology*, *12*, 45–49. https://doi.org/10.1016/J.BCAB.2017.08.015
22. Rautela, A., Rani, J., & Debnath (Das), M. (2019). Green synthesis of silver nanoparticles from Tectona grandis seeds extract: characterization and mechanism of antimicrobial action on different microorganisms. *Journal of Analytical Science and Technology*, *10*(1), 1–10. https://doi.org/10.1186/S40543-018-0163-Z/FIGURES/14
23. Rodríguez-Melcón, C., Alonso-Calleja, C., García-Fernández, C., Carballo, J., & Capita, R. (2022). Minimum Inhibitory Concentration (MIC) and Minimum Bactericidal Concentration (MBC) for Twelve Antimicrobials (Biocides and Antibiotics) in Eight Strains of Listeria monocytogenes. *Biology*, *11*(1). https://doi.org/10.3390/BIOLOGY11010046

24. Saleh, A. K., Shaban, A. S., Diab, M. A., Debarnot, D., & Elzaref, A. S. (2023). Green synthesis and characterization of aluminum oxide nanoparticles using Phoenix dactylifera seed extract along with antimicrobial activity, phytotoxicity, and cytological effects on Vicia faba seeds. *Biomass Conversion and Biorefinery*, *1*, 1–17. https://doi.org/10.1007/S13399-023-04800-X/FIGURES/10
25. Senthil, B., Devasena, T., Prakash, B., & Rajasekar, A. (2017). Non-cytotoxic effect of green synthesized silver nanoparticles and its antibacterial activity. *Journal of Photochemistry and Photobiology B: Biology*, *177*, 1–7. https://doi.org/10.1016/J.JPHOTOBIOL.2017.10.010
26. Sharma, J., Gupta, U., & Sharma, V. (2017). Modified Model for Binary Nanofluid Convection with Initial Constant Nanoparticle Volume Fraction. *Journal of Applied Fluid Mechanics*, *10*(5), 1387–1395. https://doi.org/10.18869/ACADPUB.JAFM.73.242.27754
27. Sivasubramanian, K., Tamilselvi, Y., Velmurugan, P., Oleyan Al-Otibi, F., Ibrahim Alharbi, R., Mohanavel, V., Manickam, S., Rebecca L., J., & Rudragouda Patil, B. (2024). Enhanced applications in dentistry through autoclave-assisted sonochemical synthesis of Pb/Ag/Cu trimetallic nanocomposites. *Ultrasonics Sonochemistry*, *108*, 106966. https://doi.org/10.1016/J.ULTSONCH.2024.106966
28. Sykes, J. E., & Rankin, S. C. (2013). Isolation and identification of aerobic and anaerobic bacteria. *Canine and Feline Infectious Diseases*, 17–28. https://doi.org/10.1016/B978-1-4377-0795-3.00003-X
29. Thakur, B. K., Kumar, A., & Kumar, D. (2019). Green synthesis of titanium dioxide nanoparticles using Azadirachta indica leaf extract and evaluation of their antibacterial activity. *South African Journal of Botany*, *124*, 223–227. https://doi.org/10.1016/J.SAJB.2019.05.024
30. Ulagesan, S., Nam, T. J., & Choi, Y. H. (2021). Biogenic preparation and characterization of Pyropia yezoensis silver nanoparticles (P.y AgNPs) and their antibacterial activity against Pseudomonas aeruginosa. *Bioprocess and Biosystems Engineering*, *44*(3), 443–452. https://doi.org/10.1007/S00449-020-02454-X
31. Velmurugan, P., Muruganandham, M., Sivasubramanian, K., Mohanavel, V., Chinnathambi, A., Ali Alharbi, S., & Basavegowda, N. (2024). Green synthesis of silver nanoparticles using Illicium verum extract: Optimization and characterization for biomedical applications. *Green Processing and Synthesis*, *13*(1). https://doi.org/10.1515/GPS-2023-0181/MACHINEREADABLECITATION/RIS
32. Gudkov, S. V., Burmistrov, D. E., Smirnova, V. V., Semenova, A. A., & Lisitsyn, A. B. (2022). A mini review of antibacterial properties of Al2O3 nanoparticles. *Nanomaterials*, *12*(15), 2635.
33. Manogar, P., Morvinyabesh, J. E., Ramesh, P., Jeyaleela, G. D., Amalan, V., Ajarem, J. S., ... & Vijayakumar, N. (2022). Biosynthesis and antimicrobial activity of aluminium oxide nanoparticles using Lyngbya majuscula extract. *Materials Letters*, *311*, 131569.
34. Thanaraj, S., Mitthun, A. N. K., Sravanthy, P. G., Carmelin, D. S., Surya, M., Saravanan, M., ... & MUTHUPANDIAN, S. (2024). Green synthesis of Aluminum oxide nanoparticles using Clerodendrum phlomidis and their antibacterial, anti-inflammatory, and antioxidant activities. *Cureus*, *16*(1).
35. Slavin, Y. N., Asnis, J., Hńfeli, U. O., & Bach, H. (2017). Metal nanoparticles: understanding the mechanisms behind antibacterial activity. *Journal of nanobiotechnology*, *15*, 1-20.

36. Parvekar, P., Palaskar, J., Metgud, S., Maria, R., & Dutta, S. (2020). The minimum inhibitory concentration (MIC) and minimum bactericidal concentration (MBC) of silver nanoparticles against Staphylococcus aureus. *Biomaterial investigations in dentistry*, *7*(1), 105-109.
37. Parvekar, P., Palaskar, J., Metgud, S., Maria, R., & Dutta, S. (2020). The minimum inhibitory concentration (MIC) and minimum bactericidal concentration (MBC) of silver nanoparticles against Staphylococcus aureus. *Biomaterial investigations in dentistry*, *7*(1), 105-109.
38. Adeyemi, J. O., & Fawole, O. A. (2023). Metal-based nanoparticles in food packaging and coating technologies: a review. *Biomolecules*, *13*(7), 1092.
39. Ashfaq, A., Khursheed, N., Fatima, S., Anjum, Z., & Younis, K. (2022). Application of nanotechnology in food packaging: Pros and Cons. *Journal of Agriculture and Food Research*, *7*, 100270.
40. del Rosario Herrera-Rivera, M., Torres-Arellanes, S. P., Cortés-Martínez, C. I., Navarro-Ibarra, D. C., Hernández-Sánchez, L., Solis-Pomar, F., ... & Román-Doval, R. (2024). Nanotechnology in food packaging materials: role and application of nanoparticles. *RSC advances*, *14*(30), 21832-21858.
41. Shkodenko, L., Kassirov, I., & Koshel, E. (2020). Metal oxide nanoparticles against bacterial biofilms: Perspectives and limitations. *Microorganisms*, *8*(10), 1545.
42. Ramasamy, M., & Lee, J. (2016). Recent nanotechnology approaches for prevention and treatment of biofilm-associated infections on medical devices. *BioMed Research International*, *2016*(1), 1851242.
43. Ghosh, S., Mandal, R. K., Mukherjee, A., & Roy, S. (2025). Nanotechnology in the manufacturing of sustainable food packaging: a review. *Discover Nano*, *20*(1), 36.
44. Pulizzi, F. (2016). Nanotechnology in food: Silver-lined packaging. *Nature Nanotechnology*, 1-1.

Figures

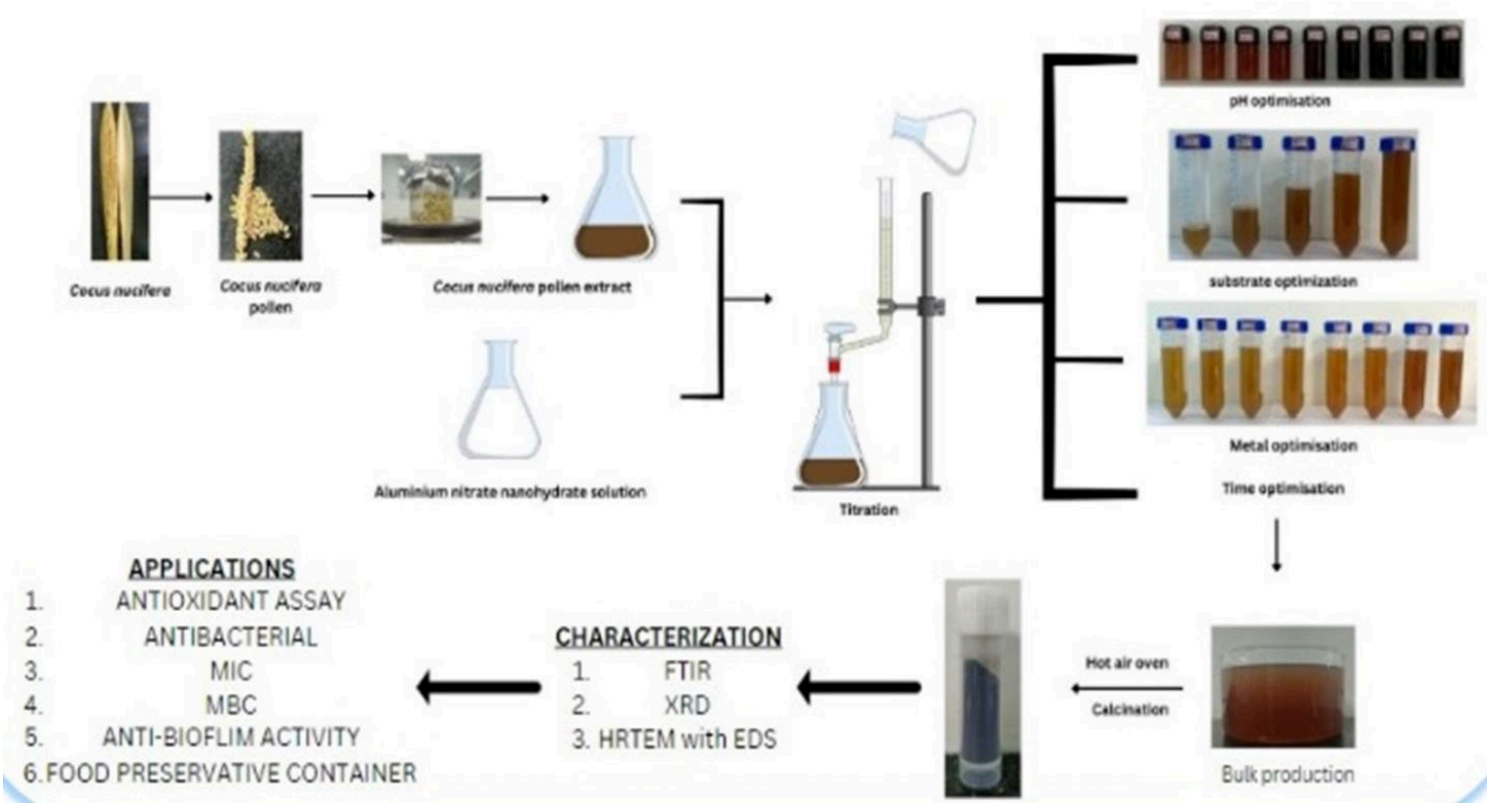

Figure 1

The schematic diagram for the biosynthesis of Al NPs using *cocos nucifera*extract and its inhibitory effect on *S.aureus,* and *E.coli* strain.

Figure 2

Fig 2.1 pH optimzation at various level

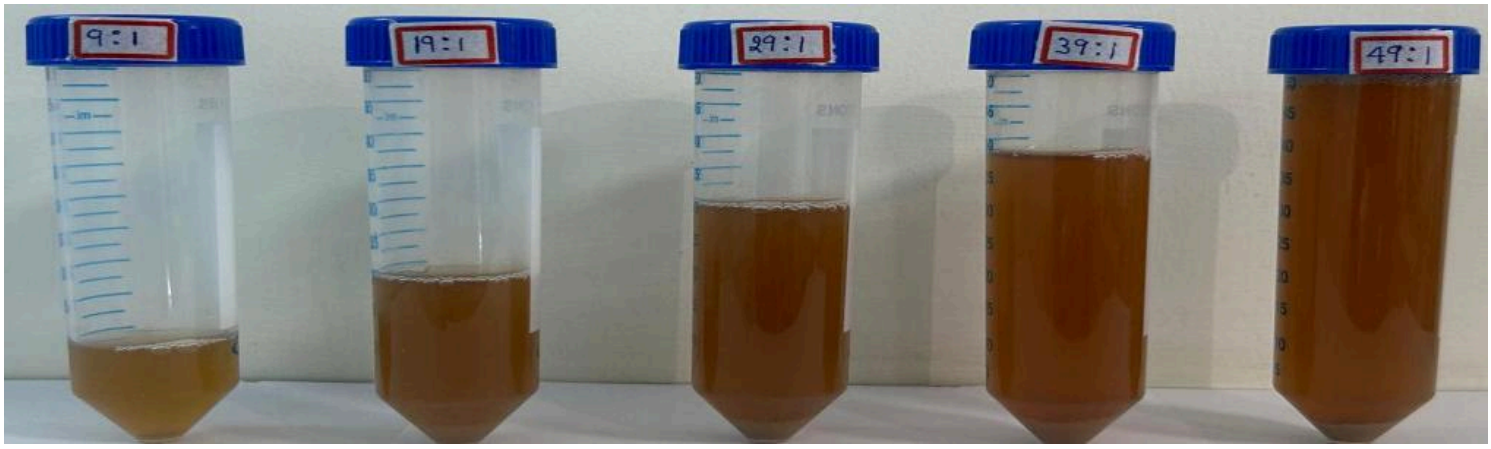

Figure 3

Fig 2.2 optimization of substrate (*cocos nucifera)*

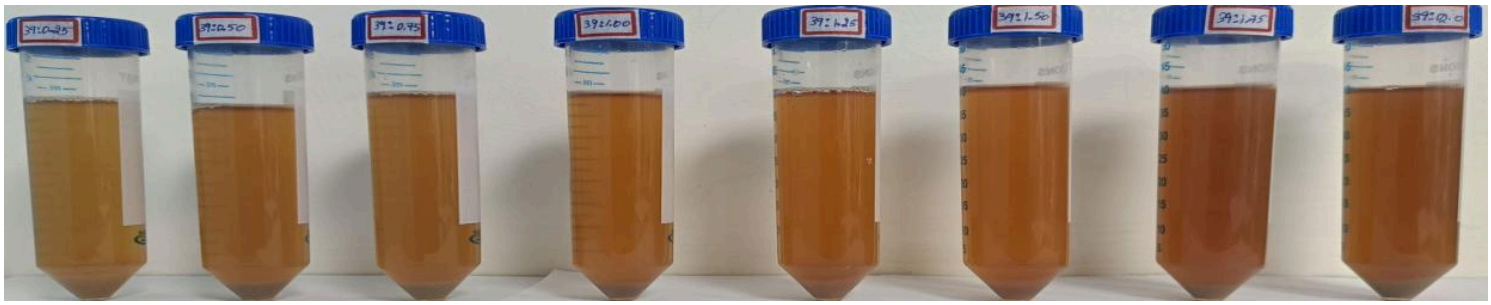

Figure 4

Fig 2.3 Optimisation of Aluminiuim metal

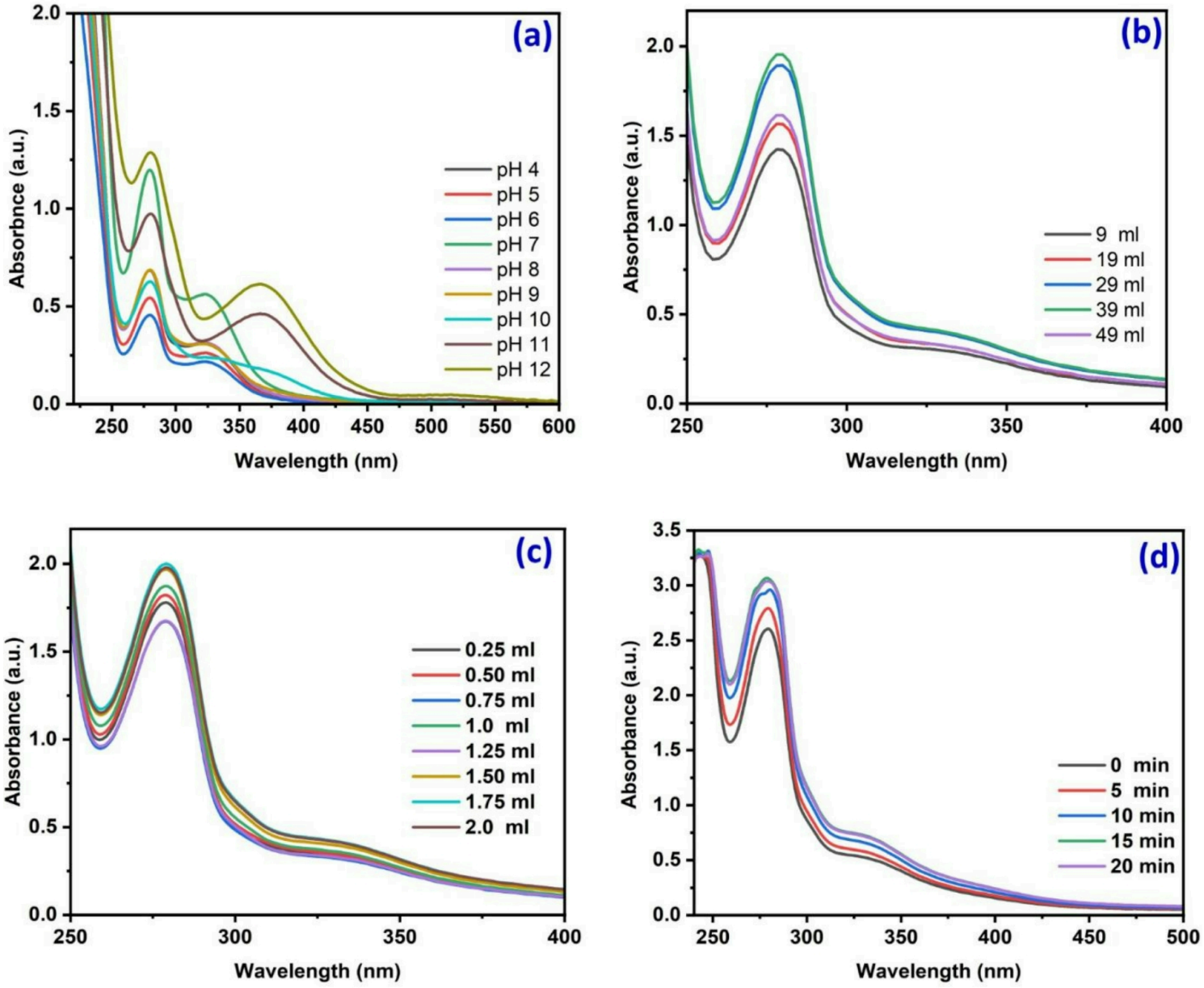

Figure 5

Fig (3a) Effect of pH on the synthesis of Al NPs, fig (3b) Effect of substrate concentration on the synthesis of Al NPs. fig (3c. Effect of Al NO_3 concentration on the synthesis of Al NPs. Fig (3d) Effect of time on the synthesis of Al NPs.

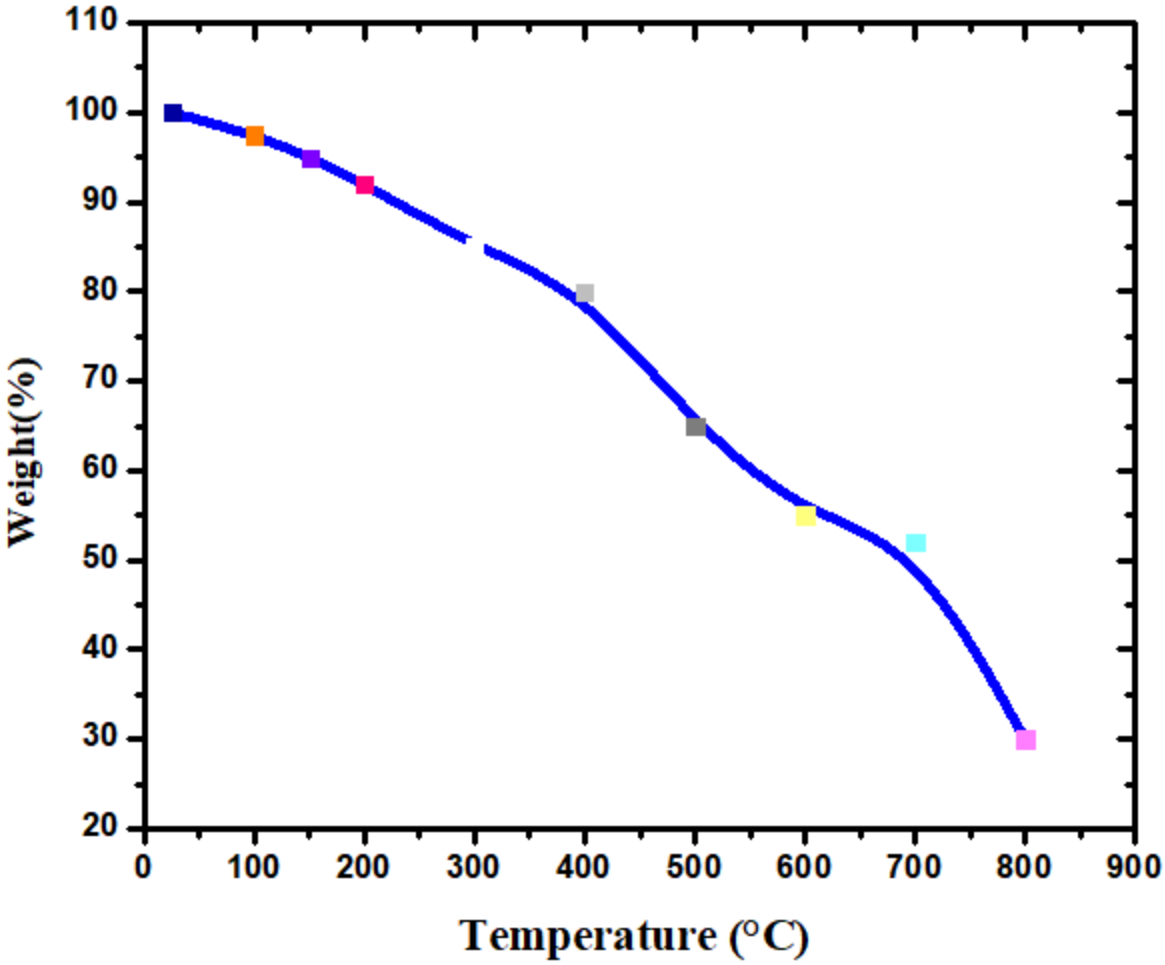

Figure 6

Fig 4 shows a TGA curve indicating that the green-synthesised AlNPs maintain their structure even at high temperatures, a notable result given their small size.

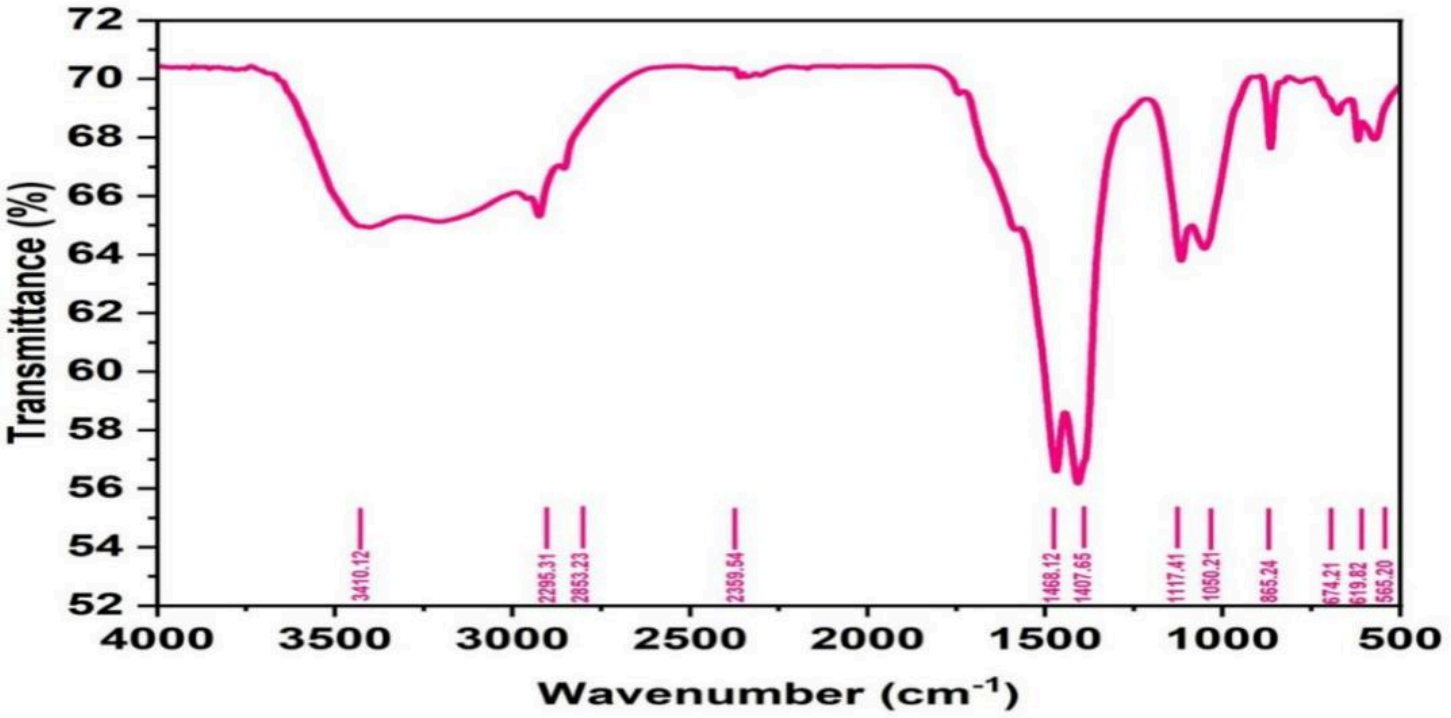

Figure 7

Fig 5 FTIR spectroscopy of synthesised Al NPs

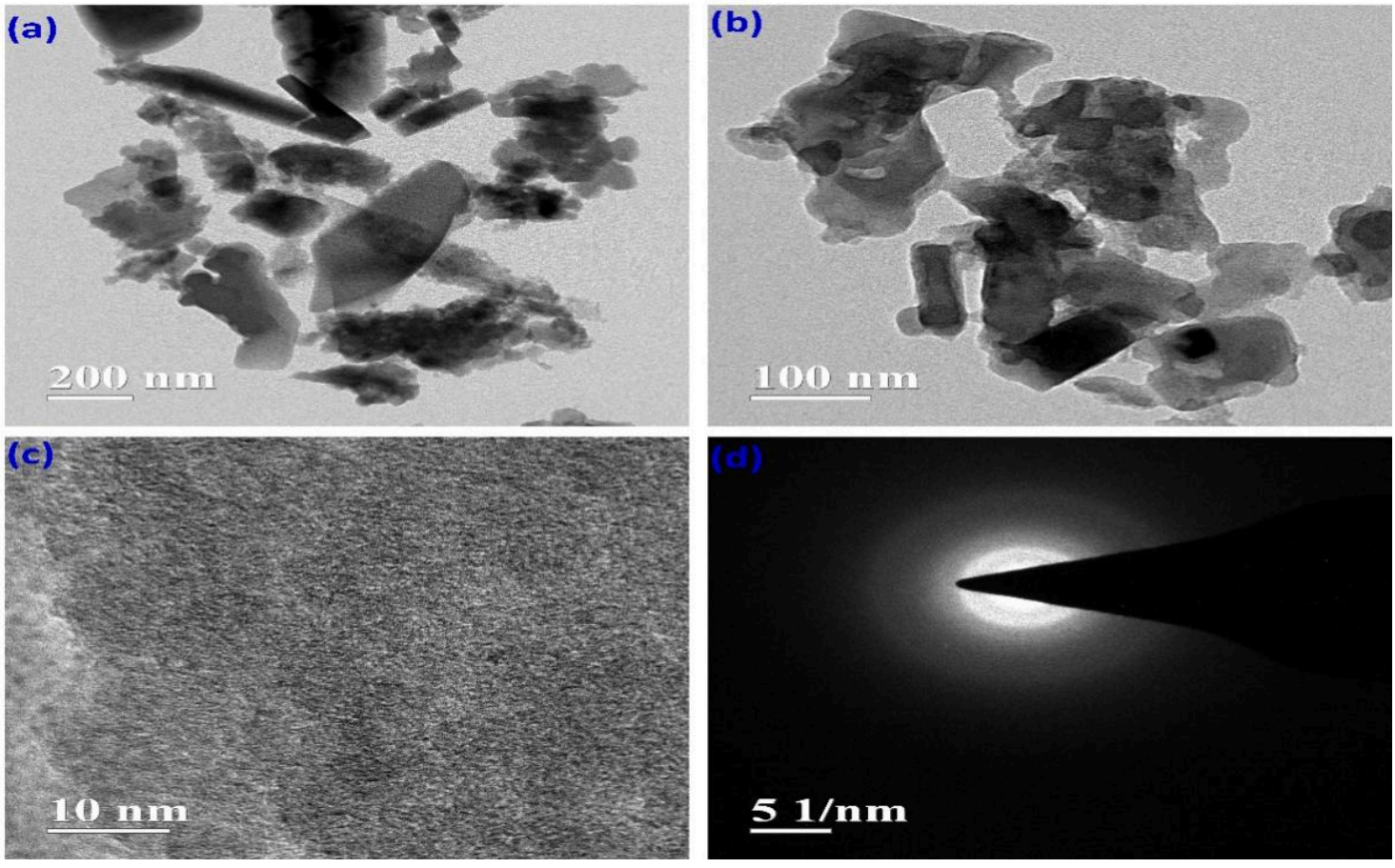

Figure 8

Fig 6(a-d) HRTEM provides clear evidence of the presence of synthesized aluminum nanoparticles. The nanoparticles vary in shape, with some being oval and others spherical. The majority of the nanoparticles were clumped together, while a few isolated particles could also be seen.

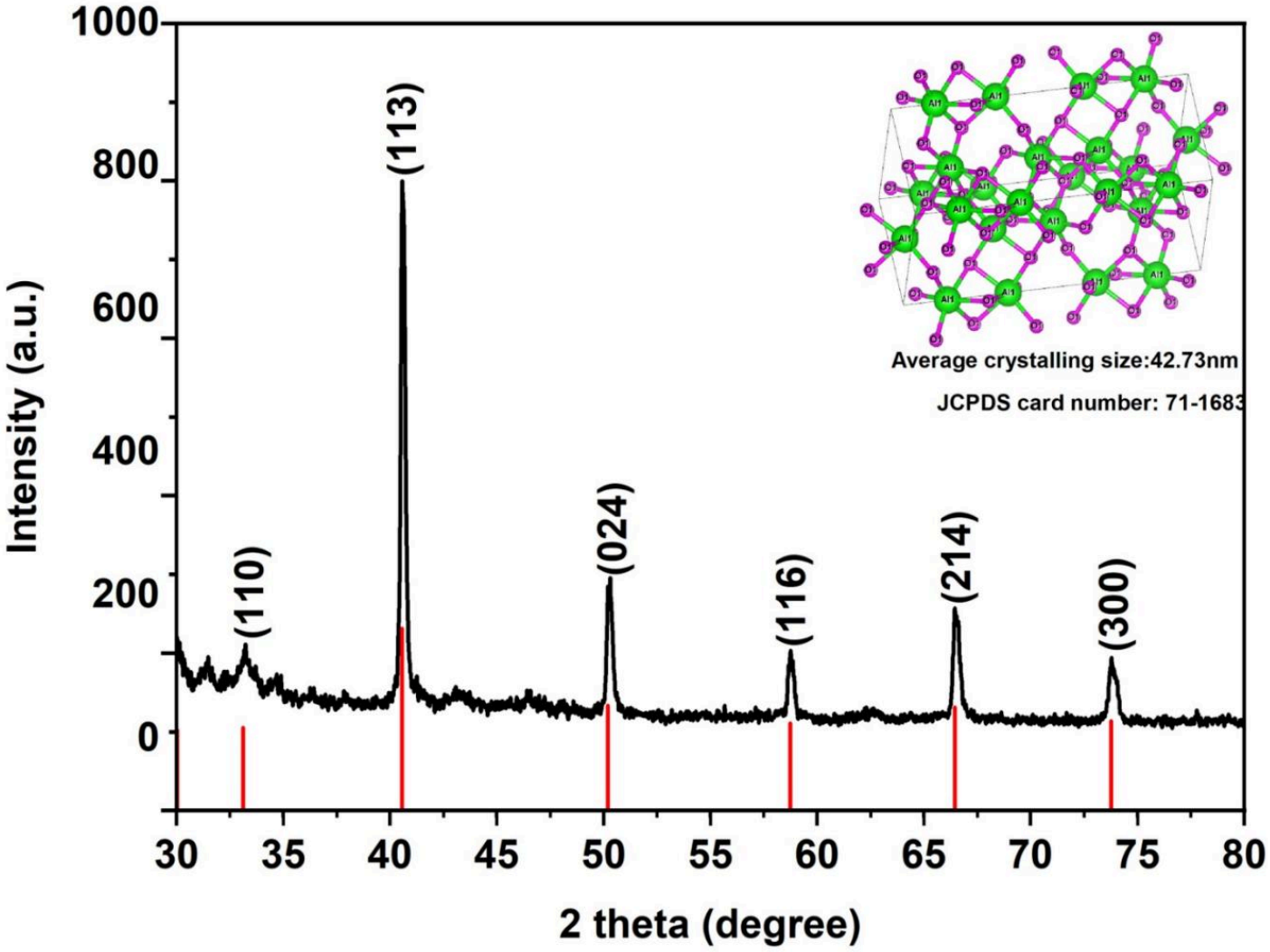

Figure 9

Fig 7 XRD pattern of synthesized aluminium nanoparticles

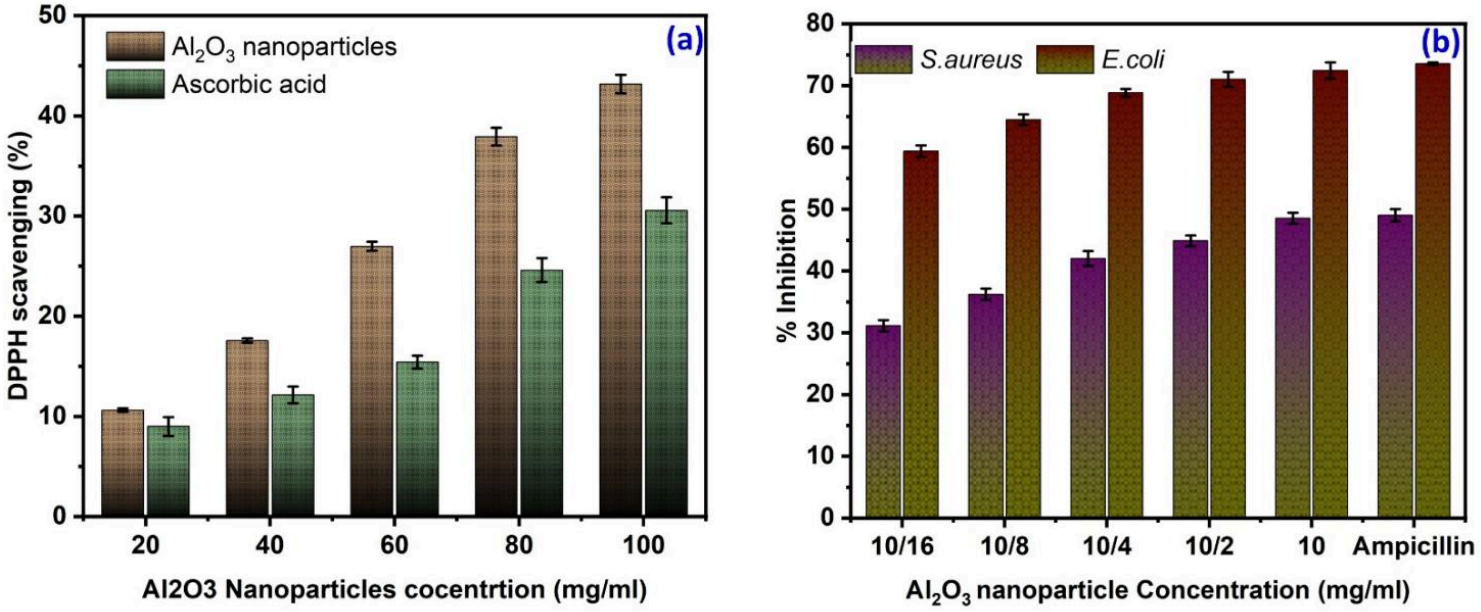

Figure 10

Fig 8a depicts the antioxidant activity assay, with aluminium nanoparticles being tested against the standard ascorbic acid. Fig 8b presents the Minimum Inhibitory Concentration of *S. aureus* and *E. coli.*

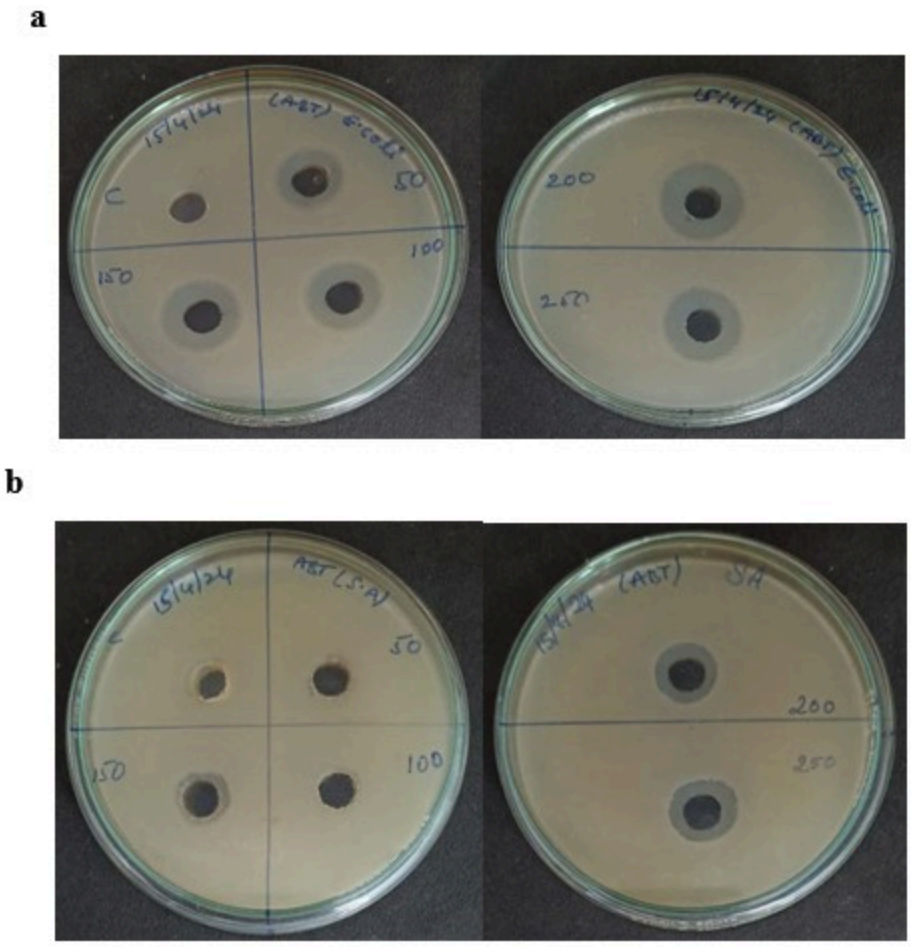

Figure 11

Fig 9 Antimicrobial activity expressed as halo zones of the Al_2O_3-NPs at different concentrations. Fig 9a Zone of inhibition (*E. coli*), Fig 9b Zone of inhibition (S. aureus).

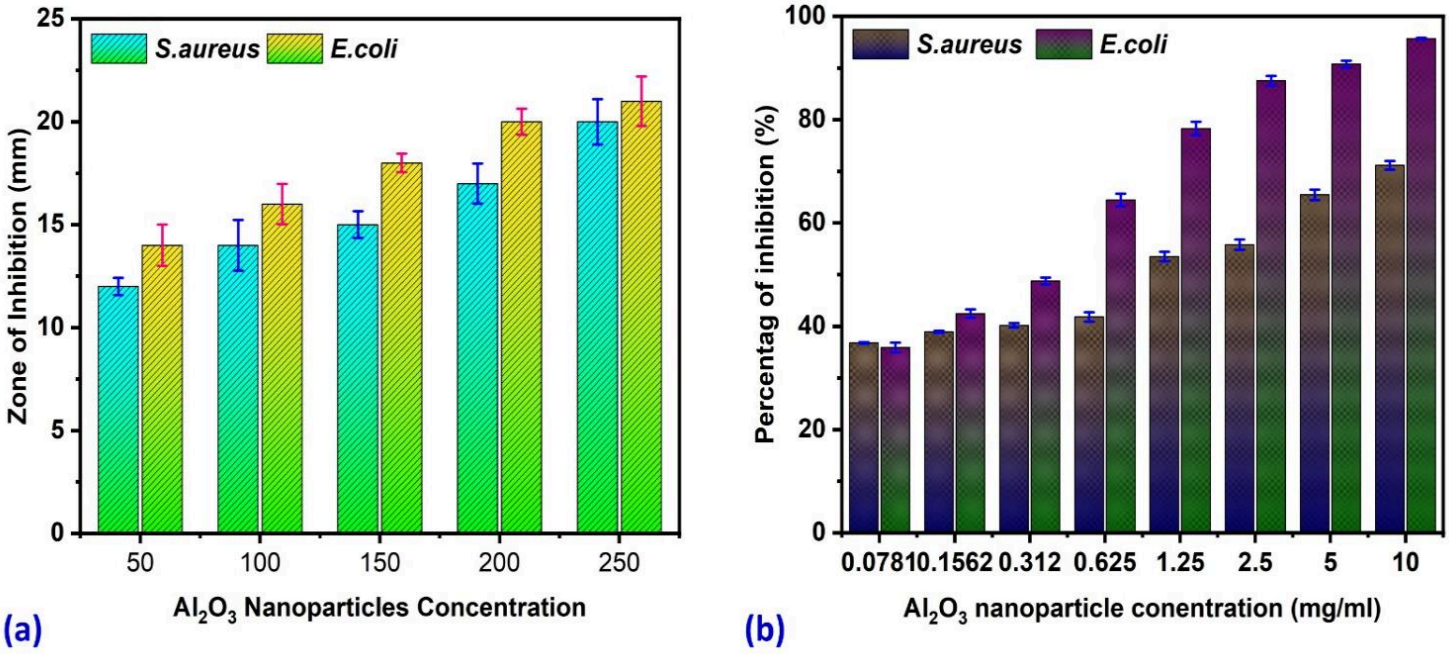

Figure 12

Fig 10a: Antibacterial activity and 10b Biofilm inhibition activity.

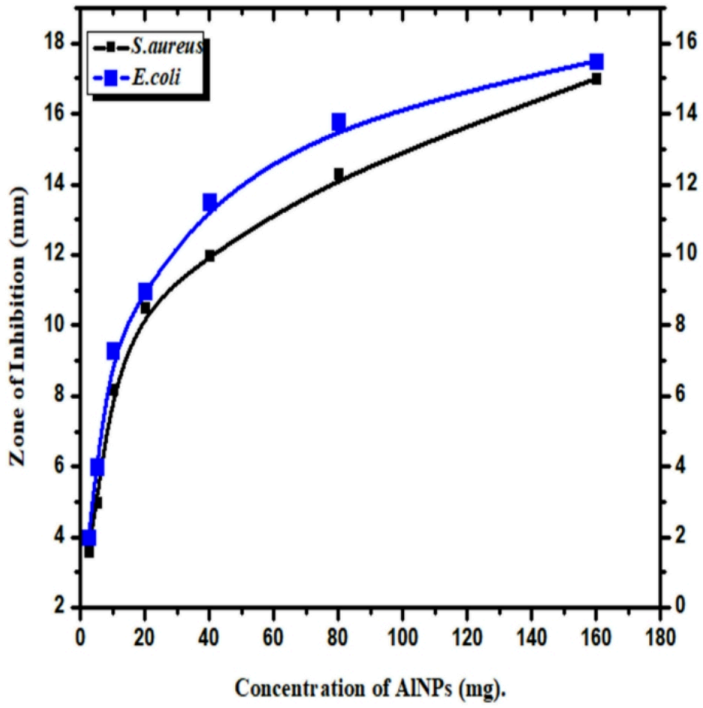

AlNPs-coated food containers exhibit varying levels of antibacterial activity, from 0 to 160 mg.

Concentration (mg)	Zone of Inhibition (E. coli) (mm)	Zone of Inhibition (S. aureus) (mm)
Control	0	0
2.5	3.6	3
5	5	4.6
10	8.2	7.3
20	10.5	9
40	12	11.5
80	14.3	13.8
160	17	15.5

Table 1 Antibacterial activity of AlNPs coated food container

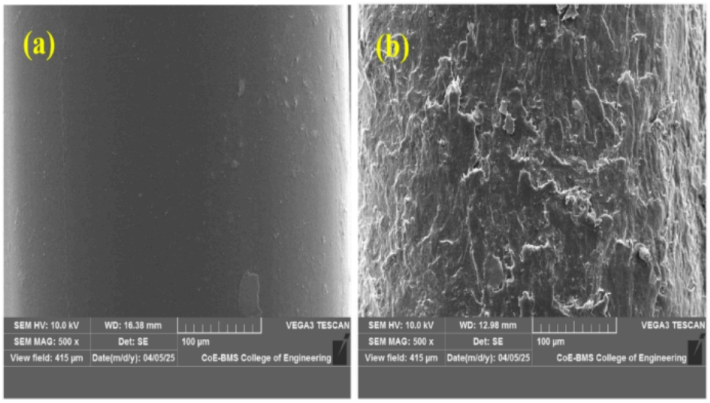

FESEM Analysis of AlNPs coated food container ((a) Before washing, (b) After washing)

Figure 13

Fig 11: AlNPs coated on food containers were tested against *S. aureus* and *E. coli* with concentrations varying from 0 to 160 mg to determine their antibacterial activity.